Boron isotope sensitivity to seawater pH change in a species of *Neogoniolithon* coralline red alga

Hannah K. Donald*[a], Justin B. Ries[b], Joseph A. Stewart[a, c], Sara E. Fowell[a], Gavin L. Foster[a]

[a] Ocean and Earth Science, National Oceanography Centre Southampton, University of Southampton Waterfront Campus, European Way, Southampton SO14 3ZH, UK

[b]Northeastern University, Marine Science Center, 430 Nahant Road, Nahant, MA 01908, USA

[c]National Institute of Standards and Technology, Hollings Marine Laboratory, 331 Fort Johnson Road, Chaarleston, SC 29412, USA

* Corresponding author (H. K. Donald). Tel.: +44 23805 96507, E-mail: h.k.donald@soton.ac.uk

The increase in atmospheric carbon dioxide (CO_2) observed since the industrial revolution has reduced surface ocean pH by ~0.1 pH units, with further change in the oceanic system predicted in the coming decades. Calcareous organisms can be negatively affected by extreme changes in seawater pH (pH_{sw}) such as this due to the associated changes in the oceanic carbonate system. The boron isotopic composition ($\delta^{11}B$) of biogenic carbonates has been previously used to monitor pH at the calcification site (pH_{cf}) in scleractinian corals, providing mechanistic insights into coral biomineralisation and the impact of variable pH_{sw} on this process. Motivated by these investigations, this study examines the $\delta^{11}B$ of the high-Mg calcite skeleton of the coralline red alga *Neogoniolithon* sp. to constrain pH_{cf}, and investigates how this taxon's pH_{cf} is impacted by ocean acidification. $\delta^{11}B$ was measured in multiple algal replicates (n = 4 to 5) cultured at four different pCO_2 scenarios – averaging (± 1σ) 409 (± 6), 606 (± 7), 903 (± 12) and 2856 (± 54) µatm, corresponding to average pH_{sw} (± 1σ) of 8.19 (± 0.03), 8.05 (± 0.06), 7.91 (± 0.03) and 7.49 (± 0.02) respectively. Results show that skeletal $\delta^{11}B$ is elevated relative to the $\delta^{11}B$ of seawater borate at all pH_{sw} treatments by up to 18 ‰. Although substantial variability in $\delta^{11}B$ exists between replicate samples cultured at a given pH_{sw} (smallest range = 2.32 ‰ at pH_{sw} 8.19, largest range = 6.08 ‰ at pH_{sw} 7.91), strong correlations are identified between $\delta^{11}B$ and pH_{sw} ($R^2 = 0.72$, $p < 0.0001$, n = 16) and between $\delta^{11}B$ and B/Ca ($R^2 = 0.72$, $p < 0.0001$, n = 16). Assuming that skeletal $\delta^{11}B$ reflects pH_{cf} as previously observed for scleractinian corals, the average pH_{cf} across all experiments was 1.20 pH units (0.79 to 1.56) higher than pH_{sw}, with the

magnitude of this offset varying parabolically with decreasing pH_{sw}, with a maximum difference between pH_{sw} and pH_{cf} at a pH_{sw} of 7.91. Observed relationships between pH_{sw} and calcification rate, and between pH_{sw} and pH_{cf}, suggest that coralline algae exhibit some resilience to moderate ocean acidification *via* increase of pH_{cf} relative to pH_{sw} in a similar manner to scleractinian corals. However, these results also indicate that pH_{cf} cannot be sufficiently increased by algae exposed to a larger reduction in pH_{sw}, adversely impacting calcification rates of coralline red algae.

1.0 Introduction

Atmospheric CO_2 has been increasing since the Industrial Revolution, from 280 ppm to more than 400 ppm today (Tans and Keeling, 2016). This increase has led to changes in ocean carbon chemistry, ultimately lowering seawater pH (pH_{sw}) by 0.1 pH units. Climate models predict that by 2100, a high-end "business as usual" emission scenario (*i.e.* Intergovernmental Panel on Climate Change: Representative Concentration Pathway 8.5) will result in a global average surface pH_{sw} of ca. 7.8, potentially reaching even lower levels at high latitudes. This large and rapid reduction in global pH_{sw} will result in an environment that is potentially challenging to marine organisms that rely on biogenically produced $CaCO_3$ (Doney et al., 2009).

Ocean acidification affects biogenic calcification by reducing the $CaCO_3$ saturation state of seawater ($\Omega = [Ca^{2+}][CO_3^{3-}]/K^*_{sp}$; where K^*_{sp} is the stoichiometric solubility product of $CaCO_3$ at in situ conditions of temperature, salinity and pressure). Reductions in Ω of seawater have been shown to reduce calcification rates and, in some cases, cause net dissolution of the calcareous shells and skeletons of marine organisms (Gattuso et al., 1998; Riebesell et al., 2000; De'ath et al., 2009; Ries et al., 2009; Ries et al., 2016). Indeed, a recent study investigating a sub-marine volcanic CO_2 seep as an analogue for the effects of ocean acidification found that, over time, the nearby coral reef system was largely replaced by fleshy algae-covered rocks (Enochs et al., 2015). This, and a wealth of other studies (Gattuso et al., 2015; and references therein), indicate

that ocean acidification can directly affect calcareous organisms through changing ocean carbonate chemistry, as well as indirectly *via* inter-species competition and modification of species interactions (*e.g.*, Dodd et al., 2015).

Coralline algae are important $CaCO_3$ producers and are often found in high latitude waters. They also comprise a large component of modern coral reefs, confer stability to the reef crest, and are a vital food source for marine grazers such as sea urchins (McCoy and Kamenos, 2015). Hence, coralline algae play an important role in the marine food web, but also act as ecosystem engineers by providing defence against coastal erosion. Coralline algae are predominantly composed of high-Mg calcite (> 15 mol % $MgCO_3$), which is more soluble than aragonite or low-Mg calcite found in other calcareous organisms such as corals, scallops and oysters (Ries et al., 2016). Since CO_2 is more soluble in colder water, it is likely that global high latitude regions are more vulnerable to ocean acidification than lower latitude regions (Gattuso et al., 2015). Thus, ocean acidification poses a severe threat to coralline algae and their interdependent ecosystems (Kuffner et al., 2008; Gao and Zheng, 2009; Ragazzola et al., 2012).

Coralline red algae calcify by depositing calcite within their cell walls, but exterior to their cell membrane. This is in contrast to foraminifera that calcify within seawater vacuoles (Erez, 2003), scleractinian corals that calcify in a fluid between their skeleton and calicoblastic epithelium (Cohen and McConnaughey, 2003; Gagnon et al., 2012), and coccolithophores that calcify in an intracellular vesicle (Mackinder et al., 2010), but is similar to calcification within *Bryopsidalean* calcareous green algae, which occurs extracellularly within interutricular space (Ries, 2009).

Several studies have examined the influence of ocean acidification on the nature and rate of calcification in a variety of coralline red algae (Hall-Spencer et al., 2008; Martin and Gattuso, 2009; Roleda et al., 2015; Cornwall et al., 2017). For instance, Ries et al. (2009) and Smith and

Roth (1979) documented a parabolic response in calcification rate of the coralline red algae to decreasing pH_{sw}, suggesting that the algal calcification increases in response to moderate elevations in pCO_2, but decreases in response to extreme increases. However, Ries et al. (2009) observed maximum calcification between pH_{sw} 7.9 and 8.1 ($\Omega_A \sim 2.0$ to 2.3; where Ω_A is the saturation state for the aragonite $CaCO_3$ polymorph), while Smith and Roth (1979) observed maximum calcification between pH_{sw} 7.6 and 8.3 (Figure 1). These non-linear relationships suggest that coralline algae utilise biological processes to confer resilience to moderate-to-extreme changes in pH_{sw}.

The calcification response of coralline algae to ocean acidification has been shown to vary between species (Borowitzka, 1981; Semesi et al., 2009; Comeau et al., 2013). Despite this, a result common to the various species investigated in the different experiments is their ability to continue calcifying, albeit at slower rates, even under extremely reduced pH_{sw}. This mitigation of extreme ocean acidification has been shown to translate into coralline algae survival in low pH_{sw} environments across a range of natural ecosystems (Kamenos et al., 2016). Coralline red algae perform both calcification and photosynthesis (*e.g.*, Buitenhuis et al., 1999), and the balance between these two key biological processes is important for coralline algae survival. Many marine organisms utilise carbon concentrating mechanisms intracellularly to ensure calcification can still occur under CO_2-limited conditions. Experimental work has shown that photosynthesis in some marine algae is CO_2-limited up to *ca.* 1000 µatm pCO_2 (Bowes, 1993). Therefore, the additional energy from photosynthesis as pCO_2 becomes elevated up to *ca.* 1000 µatm may stimulate calcification within calcifying marine algae, despite the associated decrease in pH_{sw}. This effect has previously been observed for zooxanthellate scleractinian corals (*e.g.*, Castillo et al., 2014). Furthermore, photosynthesis increases local pH through the removal of dissolved CO_2 from seawater proximal to the algae (Gao et al., 1993), and respiration may reduce calcification rates by decreasing local pH as a consequence of CO_2 release (De Beer and Larkum, 2001). Calcification in coralline algae is therefore likely regulated by a number of

important metabolic activities that influence the carbonate system within and around the algal cell (Smith and Roth, 1979; Gao et al., 1993; Hurd et al., 2011; Martin et al., 2013).

The impact of pH_{sw} and $CaCO_3$ saturation state on inorganic calcification differs from their impact on biogenic calcification (Ries et al., 2009; McCulloch et al., 2012a). The IpHRAC model by McCulloch et al. (2012b) ascribes the reduced sensitivity of scleractinian coral calcification in response to changing seawater aragonite saturation state to the increase of the calcification site pH (pH_{cf}), as determined from the boron isotopic composition of the coral skeleton, proton-sensitive microelectrodes (Ries, 2011a), and pH-sensitive dyes (Venn et al., 2013). Recent studies investigating $\delta^{11}B$ of the coralline algae *Clathromorphum nereostratum via* laser ablation inductively coupled plasma mass spectrometry (LA-ICPMS) reveal that skeletal $\delta^{11}B$ within this species is also consistent with a pH_{cf} that is significantly higher than measured ambient pH_{sw} (by ca. 0.6 pH units; $\Delta pH = pH_{cf} - pH_{sw}$), suggesting an increase of pH_{cf} may play a similarly important role in coralline algal calcification (Fietzke et al., 2015). However, skeletal $\delta^{11}B$ data for coralline algae species cultured under a range of controlled pH_{sw} conditions that demonstrate the response of pH_{cf} to changes in pH_{sw} are currently sparse (*e.g.* the only other such study is Cornwall et al., 2017). Here, the boron isotope approach to estimating pH_{cf} is applied to a branched *Neogoniolithon* sp. cultured under four pCO_2 conditions that allow us to assess the potential impacts of ocean acidification on pH_{cf} regulation in coralline red algae.

2.0 Methods

2.1 Boron isotopes

Numerous papers have presented detailed discussions about the basis for the boron isotope proxy of pH_{sw} (Hemming and Hanson, 1992; Zeebe and Wolf-Gladrow, 2001; Foster and Rae, 2016). Briefly, the proxy arises because (1) the abundance of the two major aqueous forms of boron in seawater are pH dependent and (2) there is boron isotope fractionation between these two boron species (Dickson, 1990). Trigonal planar boric acid ($B(OH)_3$) dominates at low pH,

and the tetrahedral tetrahydroxyborate anion ($B(OH)_4^-$; henceforth referred to as borate) dominates when pH exceeds 8.6 in typical surface ocean conditions. The two stable isotopes of boron (^{10}B and ^{11}B) occur roughly in a 1:4 ratio, and the structural difference between the aqueous species leads to an enrichment of ^{11}B in boric acid of approximately 27.2 ‰ (Klochko et al., 2006; Nir et al., 2015) because the more stable trigonal structure has the stronger B-O bonds. Boron isotopic composition is described using the delta notation $\delta^{11}B$ relative to a boric acid standard (NIST SRM 951 boric acid according to Catanzaro et al., 1970) shown in equation (1).

$$\delta^{11}B\ (‰) = \left[\left(\frac{^{11}B/^{10}B_{sample}}{^{11}B/^{10}B_{standard}}\right) - 1\right] \times 1000 \qquad (1)$$

Since the $\delta^{11}B$ of total boron in seawater (boric acid and borate) is constant at 39.61 ± 0.04 ‰ (Foster et al., 2010), as the proportions of boric acid and borate change with pH_{sw}, the $\delta^{11}B$ composition of each species also varies as a function of pH, with borate $\delta^{11}B$ increasing with pH_{sw} as described in equation (2).

$$\delta^{11}B_{B(OH)_4^-} = \frac{\delta^{11}B_{sw} + \left(\delta^{11}B_{sw} - 1000(\alpha_B - 1)\right) 10^{pK_B^* - pH}}{1 + \alpha_B 10^{pK_B^* - pH}} \qquad (2)$$

Where pK^*_B is the dissociation constant (dependent on temperature and salinity; Dickson, 1990), $\delta^{11}B_{sw}$ is the $\delta^{11}B$ composition of total boron in seawater, $\delta^{11}B_{B(OH)4-}$ is the $\delta^{11}B$ composition of aqueous borate, and α_B is a constant (1.0272; Klochko et al., 2006) describing the equilibrium mass dependent boron isotope fractionation between boric acid and borate.

Although borate is assumed to be the most likely form of aqueous boron incorporated into $CaCO_3$, the $\delta^{11}B$ of many biogenic carbonates is elevated relative to the $\delta^{11}B$ of seawater borate (Figure 2 and references therein; see also Vengosh et al., 1991; Gaillardet and Allègre, 1995). As noted above, this increase in the $\delta^{11}B$ of scleractinian deep-sea and tropical corals is thought to be predominantly caused by the elevation of pH_{cf} *via* enzymatic activity (*e.g.* Ca-ATPase; McConnaughey and Falk, 1991). In this case, pH_{cf} can be calculated using boron isotopes by substituting $\delta^{11}B$ of the coral sample for $\delta^{11}B$ of aqueous borate in equation (3).

$$pH = pK_B^* - log\left(-\frac{\delta^{11}B_{sw} - \delta^{11}B_{B(OH)_4^-}}{\delta^{11}B_{sw} - \alpha_B \delta^{11}B_{B(OH)_4^-} 1000(\alpha_B - 1)}\right) \quad (3)$$

Figure 2 shows $\delta^{11}B$ data from previous studies for several coral taxa grown over a range of pH_{sw} conditions (Hönisch et al., 2004; Reynaud et al., 2004; Krief et al., 2010; Anagnostou et al., 2012; McCulloch et al., 2012b; Holcomb et al., 2014). In all cases pH_{cf} is elevated by around 0.5 pH units at pH_{sw} 8, which is similar to observations of the calcifying fluid from micro-electrodes (Al-Horani et al., 2003; Krief et al., 2010; Ries, 2011a; Trotter et al., 2011; McCulloch et al., 2012b) and pH sensitive dyes (Venn et al., 2011; Venn et al., 2013; Holcomb et al., 2014). Furthermore, the majority of corals examined thus far show that as ambient pH_{sw} decreases, pH_{cf} declines at a reduced rate (Venn et al., 2011; Venn et al., 2013; Holcomb et al., 2014).

2.2 Algal Culture

A single species of tropical coralline red alga, *Neogoniolithon* sp., was cultured at four pCO_2 (± 1σ) levels: 409 (± 6), 606 (± 7), 903 (± 12) and 2856 (± 54) µatm, resulting in pH_{sw} values (± 1σ) of 8.19 (± 0.03), 8.05 (± 0.06), 7.91 (± 0.03) and 7.49 (± 0.02), respectively (Ries et al., 2009). The algae were grown for 60 days in 38 L aquaria in filtered Atlantic Ocean seawater (0.2 µm; Cape Cod, Massachusetts). The cultures were maintained at average aragonite saturation states (± 1σ) of 3.12 (± 0.22), 2.40 (± 0.42), 1.84 (± 0.13) and 0.90 (± 0.05), and temperatures of 25°C using 50 W electric heaters, and illuminated on a 10hr:14hr light:dark cycle. This species of coralline red algae exhibited an apparent parabolic calcification response to increasing pCO_2, with net calcification rate increasing with an increase in pCO_2 from 409 to 606 µatm, and declining with an increase in pCO_2 to 903 and 2856 µatm (see Ries et al., 2009 and Table SM1 in the supplementary materials for further details; Figure 1).

2.3 Sample Preparation

Neogoniolithon sp. is a non-geniculate branched rhodolith form of coralline red algae. Replicate specimens were analysed for boron isotope composition at each culture pH_{sw} (n = 5 for pH_{sw}

190 7.91, and n = 4 for pH_{sw} 8.19, 8.05 and 7.49). Duplicate analyses were performed on all replicate
191 specimens except those from the pH_{sw} 7.49 treatment, due to the small mass of $CaCO_3$
192 mineralised under these high-pCO_2 conditions. Skeletal material produced exclusively under the
193 experimental treatments was identified relative to a ^{137}Ba isotope marker emplaced in the
194 skeletons at the start of the experiment (Ries, 2011b). Branches of the specimens were
195 powdered using a pestle and mortar in a clean laboratory fitted with boron-free HEPA filters at
196 the University of Southampton to produce homogenous bulk sample replicates for each
197 specimen. Following previous studies (Foster, 2008; Krief et al., 2010), approximately 3 mg of
198 each sample was cleaned using 500 µl of an oxidative mixture of 10% hydrogen peroxide (H_2O_2)
199 buffered with 0.1 M ammonium hydroxide (NH_4OH). The samples were heated in a water bath
200 and briefly ultra-sonicated a total of six times. The oxidative mixture was removed, and the
201 samples were rinsed and transferred to clean plastic vials. The samples were leached in 0.0005
202 M nitric acid (HNO_3) and then dissolved in a minimal volume of 0.5 M HNO_3.
203
204 *2.4 Trace element and isotopic analysis*
205 Oxidatively cleaned and dissolved samples were transferred to Teflon vials and a 7% aliquot
206 was removed for trace element analysis. Elemental analysis (B/Ca and Sr/Ca) of matrix-
207 matched sample solutions was performed using ICPMS on a *Thermo Scientific Element 2* mass
208 spectrometer following the protocol of Henehan et al. (2015). Replicates of well-characterised
209 solution consistency standards measured during this study are precise to ±5.6% and ±2.0% for
210 B/Ca and Sr/Ca (95% confidence), respectively.
211
212 The remainder of each dissolved sample was reserved for boron isotope analysis and processed
213 at the University of Southampton according to well-established methods (Foster, 2008).
214 Samples were passed through micro-columns containing the boron-specific anion exchange
215 resin Amberlite IRA-743 and boron was eluted in Teflon distilled 0.5M HNO_3. Boron isotopic
216 composition of each purified sample was then measured using a *Thermo Scientific Neptune*

multi-collector ICPMS (MC-ICPMS) using two Faraday detectors fitted with 10^{12} Ω resistors at the University of Southampton following methods detailed in Henehan et al. (2013) and Foster et al. (2013). Samples were bracketed with NIST SRM 951 standard boric acid to correct for variability in instrument induced mass fractionation. The long-term reproducibility of standards is approximately ± 0.2 ‰ for 20 ng of boron (95% confidence), and analytical uncertainty is described by equation (4), where [^{11}B] is the voltage measured on the H3 faraday detector with one of the 10^{12} Ω resistors.

$$2\sigma = 12960e^{(-212[^{11}B])} + 0.3385\, e^{(-1.544\,[^{11}B])} \quad (4)$$

3.0 Results

The coralline algae across all pH treatments yield δ^{11}B values ranging from 24.42 (± 0.22) ‰ to 36.26 (± 0.10) ‰ (Table 1). One sample replicate at pH_{sw} 8.19 was deemed anomalous, as duplicate analyses differed by 1.4 ‰ compared with an average difference between other duplicate analyses of 0.18 ‰. This outlying sample is therefore excluded from the discussion, and n = 16 for all subsequent regression analyses.

The range of δ^{11}B for each pH treatment varies from 2.3 ‰ at pH_{sw} 8.19 to 6.1 ‰ at pH_{sw} 7.91. The relationship between δ^{11}B of *Neogoniolithon* sp. calcite and pH_{sw} (Figure 2) demonstrates that all δ^{11}B measurements in this study lie considerably above the pH_{sw} *vs.* aqueous borate δ^{11}B curve (Klochko et al., 2006), and are also elevated compared to other examples of biogenic carbonates thus far quantified (McCulloch et al., 2012b), with the exception of some deep-sea scleractinian corals (*e.g.* Blamart et al., 2007). The high δ^{11}B compositions observed in this study of a branching species of *Neogoniolithon* are also similar to those found in a crustose species of the same genus (Cornwall et al., 2017), suggesting that closely related species of coralline algae exhibit similar boron isotope systematics and pH_{cf}, and that growth form (*i.e.* crustose *vs.* branching) alone does not necessarily impart large differences in these systems. Although the

offset of the algae's pH_{sw} *vs.* $\delta^{11}B$ curve from the pH_{sw} *vs.* aqueous borate $\delta^{11}B$ curve is generally consistent with the offset previously observed for corals grown at various pH_{sw} (Hönisch et al., 2004; Reynaud et al., 2004; Krief et al., 2010; Anagnostou et al., 2012; McCulloch et al., 2012a; Holcomb et al., 2014), the pH_{sw} *vs.* $\delta^{11}B$ relationship for the algae is better fit (with respect to minimising residuals) with a parabolic model ($R^2 = 0.73$ and $p < 0.001$, *vs.* $R^2 = 0.53$ and $p < 0.01$ for linear fit) while the pH_{sw} *vs.* $\delta^{11}B$ relationships for corals are better fit with linear models (Trotter et al., 2011; McCulloch et al., 2012b; Holcomb et al., 2014). Details of all regressions, gradients and intercepts can be found in Table SM2 in the supplementary materials.

The measured B/Ca and $\delta^{11}B$ compositions are also highly linearly correlated ($R^2 = 0.77$, $p < 0.0001$; Figure 3A), a trend that is predicted from boron isotope systematics yet rarely observed so clearly in biogenic carbonates (Foster, 2008; Henehan et al., 2015) with the possible exception of recent work with deep-sea corals (Stewart et al., 2016). Sr/Ca has significant negative correlation with $\delta^{11}B$ ($R^2 = 0.33$, $p < 0.05$; Figure 3B).

Following the interpretations of $\delta^{11}B$ in corals (Hemming et al., 1998; Rollion-Bard et al., 2003; Allison and Finch, 2010; Rollion-Bard et al., 2011; McCulloch et al., 2012b), pH_{cf} calculated using equation 3 (assuming boron in the algal calcite is sourced solely from seawater borate) reveals an elevation of pH_{cf} relative to pH_{sw} by an average of 1.20 (± 0.22) pH units (Figure 4A). There is a statistically significant linear positive correlation ($R^2 = 0.45$, $p < 0.01$) between pH_{cf} and pH_{sw}, although once again a second-order polynomial model with an optimum near pH_{sw} 7.95 better describes the data ($R^2 = 0.66$, $p < 0.001$). If this model of boron incorporation is correct, ΔpH plotted against pH_{sw} exhibits an apparent parabolic relationship with pH_{sw} ($R^2 = 0.46$, $p < 0.01$; Figure 4B). ΔpH approaches a maximum mean of 1.26 pH units under the second most acidic treatment, and although these measurements fall within 1σ of each mean, there is a significant reduction of ΔpH at the most acidic treatment (pH_{sw} 7.49). For instance, t-tests reveal there is a

269 significant difference between the mean $\delta^{11}B$ composition of the algae cultured at pH_{sw} 8.19,
270 8.05 and 7.91 when compared to the algae cultured at pH_{sw} 7.49, confirming that a reduction in
271 pH_{sw} causes a decrease in pH_{cf} of coralline red algae.
272
273 The B/Ca of the algal specimens range from 352 (± 18) to 670 (± 84) μmol mol^{-1} (Figure 5B),
274 and is therefore comparable to B/Ca in scleractinian corals, but exceeds that found in
275 coccolithophores (Stoll et al., 2012) and foraminifera (Henehan et al., 2015). Although both
276 linear ($R^2 = 0.49$, $p < 0.01$) and second-order polynomial regressions ($R^2 = 0.72$, $p < 0.001$) of the
277 B/Ca *vs*. pH_{sw} data are statistically significant, the polynomial model better describes the data
278 (lower p-value and higher R^2). Ranges within treatments vary from 182 μmol mol^{-1} at pH_{sw} 7.91
279 to 52 μmol mol^{-1} at pH_{sw} 7.49.
280
281 Calcite Sr/Ca ranges from 2.85 (± 0.10) to 3.54 (± 0.13) mmol mol^{-1} and exhibits a statistically
282 significant negative linear correlation with pH_{sw} ($R^2 = 0.59$, $p < 0.001$; Figure 5A). A negative
283 trend is also observed between Sr/Ca and B/Ca, although it is just outside of significance at the
284 95% level ($R^2 = 0.22$, $p = 0.06$; Figure 5C).
285
286 *4.0 Discussion*
287 *4.1 $\delta^{11}B$ and B/Ca as tracers of pH*
288 The boron isotope palaeo-pH proxy has been primarily applied to foraminifera, and tropical and
289 deep-sea corals (*e.g.* Spivack et al., 1993; Sanyal et al., 1996; Palmer, 1998; Krief et al., 2010; Rae
290 et al., 2011; Anagnostou et al., 2012; Henehan et al., 2013). Calcification in foraminifera occurs
291 *via* vacuolisation of seawater (Erez, 2003; de Nooijer et al., 2014), while corals are thought to
292 biomineralise from a discrete fluid between their calicoblastic epithelium and skeleton (Cohen
293 and McConnaughey, 2003). As outlined above, calcification in coralline algae occurs
294 extracellularly within and between the cell walls of the algae yet external to their cell membrane
295 (Ries, 2009). The application of the foraminifera or coral model for the $\delta^{11}B$ proxy in coralline

algae therefore requires some key assumptions, including in particular that the algal calcification fluid has a total $\delta^{11}B$ and salinity similar to that of ambient seawater. Nonetheless, recent studies have shown that calcein, which cannot be transported across cellular membranes, is incorporated into the skeleton of the coralline algae *Lithothamnion glaciale* (Pauly et al., 2015), supporting the assumption that the site of calcification in coralline algae is at least partially open to seawater exchange (Comeau et al., 2012; Adey et al., 2013).

Regardless of the precise mechanism of calcification within this species, the strong positive correlations observed here between $\delta^{11}B$ composition, B/Ca ratio and pH_{sw} indicate that boron systematics of coralline algae do vary with respect to pH_{sw}. As expected from the existing understanding of the proxy, cultures at lower pH_{sw} have lower $\delta^{11}B$ and B/Ca; both, in theory, resulting from a reduction in borate concentration relative to boric acid at lower pH_{sw}. Nonetheless, the $\delta^{11}B$ data for the coralline algae presented here plot well above the borate $\delta^{11}B$ *vs.* pH_{sw} curve. Therefore, following the model for boron isotopes in corals proposed by McCulloch et al., (2012a), the results of our study suggest that coralline algae substantially increase pH_{cf} to promote calcification. Indeed pH_{cf} has been shown to increase during seasonal variations in ΔpH of 0.5 to 0.7 pH units within the coralline algae species *Clathromorphum nereostratum* (Fietzke et al., 2015), and the more recent study by Cornwall et al. (2017) shows that a crustose species of the *Neogoniolithon* genus exhibits a ΔpH of ca. 0.8 – 1.1 pH units, depending on pH_{sw}.

Interpreting the results of the boron isotope data presented here following standard boron isotope pH proxy assumptions that (1) boron enters the algal calcification site unfractionated from seawater, (2) boron isotope fractionation in coralline algae is controlled only by pH_{cf}, and (3) only seawater borate is incorporated into the coralline algal skeleton, suggests that *Neogoniolithon* sp. undergoes a large pH_{cf} increase of, on average, 1.20 units (Figure 4). In light of these findings, and the unique calcification mechanism in coralline algae compared to other

marine calcifiers, some alternative models of boron systematics within coralline algae should be explored to ensure that these standard assumptions are met in coralline algae. The impact of possible boric acid incorporation, and Rayleigh fractionation of the calcifying medium and other processes affecting coralline algal skeletal chemistry are discussed in the following sections.

4.1.1 Boric acid incorporation

Isotopically heavy boric acid has a similar size and the same trigonal planar structure as the carbonate ion (CO_3^{2-}) found in the algal calcite lattice and, whilst boric acid holds no charge, it may be incorporated as an impurity. Solid state ^{11}B nuclear magnetic resonance (NMR) spectroscopy on coralline algal calcite has revealed that approximately 30% of boron is present in a trigonal geometry, and Cusack et al. (2015) suggested that boric acid may therefore be directly incorporated into the high-Mg calcite of *Neogoniolithon* sp. The incorporation of ^{11}B enriched boric acid into the calcite lattice would result in higher skeletal $\delta^{11}B$. Therefore, boric acid incorporation may partially explain the positive shift in skeletal $\delta^{11}B$ compositions (relative to $\delta^{11}B$ of seawater borate) that we report here (Figure 2).

Assuming that both seawater borate and boric acid are incorporated into coralline algal calcite, the proportion of boric acid required to match the mean skeletal $\delta^{11}B$ compositions of the algae is between 44 and 60% (Table 2), thereby greatly exceeding the ~30% suggested from *in situ* ^{11}B MAS NMR studies (Cusack et al., 2015), yet it should also be noted that Cusack et al. (2015) examined a different species of coralline algae (*Lithothamnion glaciale*). Furthermore, given that the abundance of boric acid is pH dependent, it would be expected that the percentage of boric acid incorporated should increase with decreasing pH_{sw} (*i.e.* with increasing boric acid in solution; Noireaux et al., 2015). This was not observed for the specimens of *Neogoniolithon* sp. investigated here, as the percentage of boric acid incorporation required to explain the ^{11}B enrichment levels off for the two lowest pH_{sw} treatments.

^{11}B NMR studies by Mavromatis et al. (2015) and Noireaux et al. (2015) have recently shown that inorganically precipitated calcite contains up to 65% trigonal boron, although a linear relationship between pH_{sw}, and measured $\delta^{11}B$ of the calcite was maintained. However, these studies did identify a significant relationship between the percentage of trigonal boron in the lattice and calcite growth rate. Noireaux et al. (2015) observed that slow growth rate led to a higher percentage of trigonal boron in the calcite lattice, and suggested that this indicates an increase in boric acid incorporation (see also Mavromatis et al., 2015). The slowest growth rates in our cultured *Neogoniolithon* sp. are found at pH_{sw} 8.19 and 7.49, where in contrast, our boron isotope data suggests the smallest boric acid incorporation (Table 2). In light of these findings, it seems unlikely that boric acid incorporation is a dominant driver of the heavy $\delta^{11}B$ (relative to $\delta^{11}B$ of aqueous borate expected at that pH_{sw}) observed in cultured *Neogoniolithon* sp., or has a significant influence on the relationship between skeletal $\delta^{11}B$ and pH_{sw} in this species. Furthermore, although ^{11}B NMR studies may reveal that trigonal boron is present in the calcite lattice, this may be a result of geometry change of the borate molecule during incorporation into the calcite lattice, rather than direct incorporation of boric acid (Balan et al., 2016).

4.1.2 Rayleigh fractionation

Coralline algae calcification occurs intercellularly within the cell walls of the algae, which are semi-isolated from seawater by adjacent cells. Nevertheless, these extracellular restricted environments are likely to be permeable to seawater and maintained at elevated pH and calcite saturation state to promote calcification. Rayleigh fractionation describes the process by which molecules or ions are continuously removed from a closed or semi-closed system, leading to progressive change in the elemental and/or isotopic composition of the residual fluid. The precipitation of $CaCO_3$ in this semi-isolated calcification space may therefore lead to changes in the elemental and isotopic composition of the algal calcite (as proposed for corals by Gaetani and Cohen, 2006; Gagnon et al., 2007). For example, assuming that borate (isotopically lighter

than total seawater boron) is solely incorporated into coralline algal calcite, the remaining fluid would become enriched in ^{11}B, imposing a heavier $\delta^{11}B$ composition on the later forming calcite.

The partition coefficient (K_D) of boron into calcite is described by equation (5).

$$K_D = \frac{[B/Ca]_{CaCO_3}}{[B/Ca]_{seawater}} \quad (5)$$

There are several estimates for the K_D of boron, and all are much less than one (*ca.* 0.0005; Yu et al., 2007; Stoll et al., 2012). Consequently, as calcification progresses, Rayleigh fractionation drives an increase in the B/Ca ratio of the residual fluid, thereby increasing B/Ca of the latterly precipitated $CaCO_3$. In theory, therefore, Rayleigh fractionation may be sufficient to describe both the observed enrichment in ^{11}B in coralline algae calcite relative to seawater borate (Figure 2), the observed relationships between pH_{sw} and both coralline algal B/Ca (Figure 5) and $\delta^{11}B$ (Figure 2), as well as the observed correlation between coralline algal B/Ca and $\delta^{11}B$ (Figure 3).

However, the study of boron incorporation into deep sea scleractinian corals by Stewart et al. (2016) shows that Rayleigh fractionation is unable to drive significant changes in skeletal $\delta^{11}B$ and B/Ca from unmodified seawater (*i.e.* [B] of 432 μmol kg^{-1}; [Ca] of 10.3 mmol kg^{-1}; salinity 35 psu) given a typical biogenic carbonate B/Ca of ~600 μmol mol^{-1} because insufficient borate is removed at each incremental step of precipitation to drive the observed change in $CaCO_3$ $\delta^{11}B$. Thus Rayleigh fractionation can only explain the relationship observed in Figure 3 between B/Ca and $\delta^{11}B$ if the B/Ca ratio of the calcifying fluid is very much reduced relative to that of seawater and the partition coefficient is higher than estimates from inorganic experiments (in order to maintain the observed B/Ca ratio). For instance, a Rayleigh model fitted to the $\delta^{11}B$ and B/Ca data in this study suggests a high K_D of 0.5, and a 98.5% reduction in seawater boron content at the site of calcification. While this is a possibility in coralline algae as calcification occurs within a semi-restricted space, the inverse correlation between Sr/Ca and B/Ca when both elements have a K_D of <1 within calcite (defined in equation 5; Figure 5), suggests that

Rayleigh fractionation is unlikely to account for the entirety of the observed ^{11}B enrichment in *Neogoniolithon* sp. relative to seawater borate, as well as the observed relationships between pH_{sw} and $\delta^{11}B$, and B/Ca.

4.2 Calcification rate and implications for coralline red algae in a high-CO_2 world

Boron isotope characteristics of *Neogoniolithon* coralline red algae are unlikely to result from boric acid incorporation or Rayleigh fractionation. Recent inorganic precipitation experiments have highlighted the importance of calcification rate in controlling B/Ca in calcite (Gabitov et al., 2014; Mavromatis et al., 2015; Noireaux et al., 2015; Uchikawa et al., 2015). Here we find strong correlation between calcification rate and B/Ca ($R^2 = 0.40$, $p < 0.01$), which is therefore entirely consistent with pH_{cf} elevation increasing Ω and borate concentration at the site of calcification, thereby driving increased boron incorporation into the algal calcite. Although this might be expected to also increase Sr/Ca given inorganic experiments (*e.g.* Böhm et al., 2012), the Sr/Ca in the cultured coralline algae exhibits a positive correlation with DIC (umol $kgsw^{-1}$; Figure SM1A); a relationship recently documented in foraminifera (Keul et al., 2017). This points towards a new proxy in coralline algae that has potential to fully resolve the carbonate system.

We are then left with the possibility that $\delta^{11}B$ of the algal calcite reflects pH_{cf} pursuant to the $\delta^{11}B$-pH_{sw} relationship, as proposed for scleractinian corals (e.g. McCulloch et al., 2012b). Since pH_{cf} will largely control calcite saturation state (Ω) at the site of calcification, calcification rate should exhibit a strong relationship with $\delta^{11}B$ and pH_{cf}. This is apparent when calcification rates of individual algal specimens (Ries et al., 2009) are plotted against their respective $\delta^{11}B$-derived values of pH_{cf} (Figure 6A). The observed relationship between coralline algal calcification rate and pH_{sw} (Figure 6B; *i.e.*, increased calcification under slightly elevated pCO_2, reduced calcification at extremely elevated pCO_2; Ries et al., 2009) may thus arise from the relationship between pH_{sw} and pH_{cf} (Figure 4). Furthermore, the ability of *Neogoniolithon* algae to raise pH_{cf} relative to pH_{sw} increases under more acidified conditions, with ΔpH increasing from 0.85 (±

430 0.11) to 1.26 (± 0.22) between pH_{sw} of 8.19 to 7.91. These results are consistent with three
431 coralline algae species (including a crustose *Neogoniolithon* sp.) cultured at variable pH_{sw} by
432 Cornwall et al. (2017), which also exhibit a similar increase in ΔpH from ca. 0.8 to ca. 1.1
433 between pH_{sw} of 8.08 to 7.64 (Cornwall et al., 2017). However, our observation that ΔpH
434 levelled off under the two most acidic treatments suggests that there is a limit to the extent to
435 which the branching species of *Neogoniolithon* can elevate pH_{cf} relative to pH_{sw}. This limit may
436 also exist for those species examined by Cornwall et al. (2017) but is not resolvable because
437 their pH_{cf} data are confined to a narrower pH_{sw} range, with only three pH_{sw} treatments
438 examined that fall within the linear portion of our pH_{cf} *vs.* pH_{sw} relationship. Nonetheless, taken
439 together, our study and that of Cornwall et al. (2017) illustrate that pH_{cf} in coralline algal
440 therefore appears to promote calcification in moderately acidified seawater (down to pH_{sw}
441 7.95), which is most likely due to CO_2-fertilisation of photosynthesis. This supports the previous
442 observation that photosynthesis in some marine algae is CO_2-limited up to *ca.* 1000 µatm pCO_2
443 (Bowes, 1993). Our new data at low pH_{sw}, however, reveals that no additional benefit for
444 photosynthesis in this coralline alga appears to be conferred by increasing pCO_2 from 903 to
445 2856 µatm pCO_2, while the accompanying increase in acidity and resulting decrease in Ω of the
446 culture solution has a clear detrimental effect on the calcification rate of the algae.
447
448 As has been demonstrated for scleractinian corals (McCulloch et al., 2012b), the ability of
449 coralline algae to elevate pH_{cf} may confer resilience to the deleterious effects of ocean
450 acidification, thereby giving them an advantage over calcifying taxa competing for space on the
451 seafloor that lack this ability. Specifically, our data suggest that species-specific pH_{sw} optima
452 exist at pH_{sw} ca. 8 for maximising both pH_{cf} and calcification rates of *Neogoniolithon* sp.
453 However, that pH_{cf} and algal calcification rates begin to dramatically decline as pH_{sw} is
454 decreased from 7.9 to 7.5 indicates that there are limits to the extent that coralline algae can
455 mitigate the effects of more extreme ocean acidification. Indeed, at extremely low pH_{sw},
456 mineralogical changes (high Mg calcite to gypsum ratio) are induced in other species of coralline

algae (Kamenos et al., 2016). Together, these findings have implications for how *Neogoniolithon* sp. will cope with increasing ocean acidification in the future.

4.3 Intra-treatment variability and implications for the boron isotope proxy

One notable feature of the $\delta^{11}B$ presented here for *Neogoniolithon* sp. is the degree of variability between specimen replicates within pH_{sw} treatments. Although some degree of scatter between replicates is often observed in other culture studies, in this case it reached ca. 6 ‰. Some of this scatter may be influenced by the heterogeneity of the bulk samples, as microstructural differences have been shown to affect $\delta^{11}B$ in aragonitic corals by up to 10 ‰ (Blamart et al., 2007), and laser ablation $\delta^{11}B$ has revealed variations of up to 6 ‰ in other species of coralline algae (Fietzke et al., 2015). That the spread in $\delta^{11}B$ is still fairly large at the pH_{sw} closest to ambient confirms this is not a methodological artefact where pre-experimental skeleton is inadvertently sampled, but rather is a primary feature of this species of coralline red algae. This is also confirmed by the lack of correlation between the scatter from the mean $\delta^{11}B$ for each treatment and the mass of $CaCO_3$ measured (Figure SM2).

Despite this spread in $\delta^{11}B$ for a given treatment, there remains good correlation between B/Ca and $\delta^{11}B$ (Figure 3). Although the strength of this correlation is perhaps unexpected given some related studies (e.g. Douville et al., 2010; Henehan et al., 2015), this further supports the assertion that coralline algal calcification rate, $\delta^{11}B$ and B/Ca are controlled by pH_{cf} of the algae, and that there is considerable variability in pH_{cf} amongst individuals.

The finding that coralline red algal $\delta^{11}B$ responds to pH_{sw} suggests that this is a potential taxon for reconstructing palaeo-pH_{sw}; a conclusion that is particularly noteworthy given coralline algae's ability to produce long growth records in high-latitude oceans, where palaeo-pH_{sw} records are sparse (Fietzke et al., 2015). Despite these encouraging results, further work on *Neogoniolithon* is clearly required to determine whether the $\delta^{11}B$ of this genus of coralline algae

offers the precision and accuracy needed to reliably reconstruct past changes in pH_{sw}, particularly in light of their strong inter-specimen variability in boron geochemistry.

5.0 Conclusion

We find that statistically significant relationships exist in cultures of the coralline red algae *Neogoniolithon* sp. between $\delta^{11}B$ and pH_{sw}, $\delta^{11}B$ and skeletal B/Ca, and pH_{cf} and net calcification rate. Skeletal $\delta^{11}B$ in this species is considerably elevated compared to $\delta^{11}B$ of both seawater borate and most other examples of biogenic carbonate, suggesting an average pH_{cf} increase of more than 1 pH unit relative to pH_{sw}. An observed correlation between calcification rate and pH_{cf} suggests that the algae promote calcification by elevating pH_{cf}. Furthermore, the observation that ΔpH increased as pH_{sw} decreased from 8.2 to 7.9 suggests that this species of coralline red algae is able to mitigate the effects of moderate ocean acidification *via* pH regulation at the site of calcification. However, the observation that pH_{cf} and calcification rates decreased when pH_{sw} was reduced to 7.5 suggest that there is a limit to the extent to which this species can mitigate the effects of extreme ocean acidification.

Acknowledgements

Financial support for this study was provided by the Natural Environmental Research Council (UK) to H.K.D. (grant number 1362080) and G.L.F. (NE/H017356/1). J.B.R. acknowledges funding from NSF-BIO-OCE 1437371 and NSF-BIO-OCE 1459706 and acknowledges Northeastern University's Marine Science Center. We thank J. A. Milton and M. J. Cooper (University of Southampton) for their assistance during MC-ICPMS work. Discussions with A. J. Poulton and C. M. Moore are gratefully acknowledged. The authors also thank associate editor Claire Rollion-Bard, and three reviewers (Nick Kamenos and two anonymous) for their constructive feedback that led to an improved version of this manuscript.

References

Adey W. H., Halfar J. and Williams B. (2013) Biological, Physiological, and Ecological Factors Controlling Carbonate Production in an Arctic-Subarctic Climate Archive. *Smithson. Contrib. Mar. Sci.*, 1–41.

Al-Horani F. a, Al-Moghrabi S. M. and De Beer D. (2003) The mechanism of calcification and its relation to photosynthesis and respiration in the scleractinian coral *Galaxea fascicularis*. *Mar. Biol.* **142**, 419–426.

Allison N. and Finch A. A. (2010) δ11B, Sr, Mg and B in a modern *Porites* coral: the relationship between calcification site pH and skeletal chemistry. *Geochim. Cosmochim. Acta* **74**, 1790–1800.

Anagnostou E., Huang K. F., You C. F., Sikes E. L. and Sherrell R. M. (2012) Evaluation of boron isotope ratio as a pH proxy in the deep sea coral *Desmophyllum dianthus*: Evidence of physiological pH adjustment. *Earth Planet. Sci. Lett.* **349–350**, 251–260.

Balan E., Pietrucci F., Gervais C., Blanchard M., Schott J. and Gaillardet J. (2016) First-principles study of boron speciation in calcite and aragonite. *Geochim. Cosmochim. Acta* **193**, 119–131.

De Beer D. and Larkum A. W. D. (2001) Photosynthesis and calcification in the calcifying algae *Halimeda discoidea* studied with microsensors. *Plant, Cell Environ.* **24**, 1209–1217.

Blamart D., Rollion-Bard C., Meibom A., Cuif J. P., Juillet-Leclerc A. and Dauphin Y. (2007) Correlation of boron isotopic composition with ultrastructure in the deep-sea coral *Lophelia pertusa*: Implications for biomineralization and paleo-pH. *Geochemistry, Geophys. Geosystems* **8**, 1–11.

Böhm F., Eisenhauer A., Tang J., Dietzel M., Krabbenhöft A., Kisakürek B. and Horn C. (2012) Strontium isotope fractionation of planktic foraminifera and inorganic calcite. *Geochim. Cosmochim. Acta* **93**, 300–314.

Borowitzka M. A. (1981) Photosynthesis and calcification in the articulated coralline red algae *Amphiroa anceps* and *A. foliacea*. *Mar. Biol.* **62**, 17–23.

Bowes G. (1993) Facing the inevitable: Plants and increasing atmospheric CO2. *Annu. Rev. Plant Physiol. Plant Mol. Biol.* **44**, 309–32.

Buitenhuis E. T., De Baar H. J. W. and Veldhuis M. J. W. (1999) Photosynthesis and Calcification By *Emiliania Huxleyi* (*Prymnesiophyceae*) As a Function of Inorganic Carbon Species. *J. Phycol.* **35**, 949–959.

Castillo K. D., Ries J. B., Bruno J. F. and Westfield I. T. (2014) The reef-building coral *Siderastrea siderea* exhibits parabolic responses to ocean acidification and warming. *Proc. Biol. Sci.* **281**, 20141856–20141856.

Catanzaro E. J., Champion C. E., Garner E. L., Marinenko G., Sappenfield K. M. and Shields W. R. (1970) *Boric Acid: Isotopic and Assay Standard Reference Materials*., NBS (US) Special Publications, National Bureau of Standards, Institute for Materials Research, Washington, D. C.

Cohen A. L. and McConnaughey T. A. (2003) Geochemical Perspectives on Coral Mineralization. *Rev. Mineral. Geochemistry* **54**, 151–187.

Comeau S., Carpenter R. C. and Edmunds P. J. (2012) Coral reef calcifiers buffer their response to ocean acidification using both bicarbonate and carbonate. *Proc. R. Soc. B Biol. Sci.* **280**, 20122374–20122374.

Comeau S., Edmunds P. J., Spindel N. B. and Carpenter R. C. (2013) The responses of eight coral reef calcifiers to increasing partial pressure of CO 2 do not exhibit a tipping point. *Limnol. Oceanogr.* **58**, 388–398.

Cornwall C. E., Comeau S. and Mcculloch M. T. (2017) Coralline algae elevate pH at the site of calcification under ocean acidification. *Glob. Chang. Biol.* **0**, 1–12.

Cusack M., Kamenos N. A., Rollion-Bard C. and Tricot G. (2015) Red coralline algae assessed as marine pH proxies using 11B MAS NMR. *Sci. Rep.* **5**, 8175.

De'ath G., Lough J. M. and Fabricius K. E. (2009) Declining coral calcification on the Great Barrier Reef.

Science (80-.). **323**, 116–119.

Dickson A. G. (1990) Thermodynamics of the dissociation of boric acid in synthetic seawater from 273.15 to 318.15 K. *Deep Sea Res.* **37**, 755–766.

Dodd L. F., Grabowski J. H., Piehler M. F., Westfield I. and Ries J. B. (2015) Ocean acidification impairs crab foraging behaviour. *Proc. Biol. Sci.* **282**, 20150333.

Doney S. C., Fabry V. J., Feely R. A. and Kleypas J. A. (2009) Ocean Acidification: The Other CO2 Problem. *Ann. Rev. Mar. Sci.* **1**, 169–192.

Douville E., Paterne M., Cabioch G., Louvat P., Gaillardet J., Juillet-Leclerc A. and Ayliffe L. (2010) Abrupt sea surface pH change at the end of the Younger Dryas in the central sub-equatorial Pacific inferred from boron isotope abundance in corals (*Porites*). *Biogeosciences* **7**, 2445–2459.

Enochs I. C., Manzello D. P., Donham E. M., Kolodziej G., Okano R., Johnston L., Young C., Iguel J., Edwards C. B., Fox M. D., Valentino L., Johnson S., Benavente D., Clark S. J., Carlton R., Burton T., Eynaud Y. and Price N. N. (2015) Shift from coral to macroalgae dominance on a volcanically acidified reef. *Nat. Clim. Chang.*, 1–9.

Erez J. (2003) The Source of Ions for Biomineralization in Foraminifera and Their Implications for Paleoceanographic Proxies. *Rev. Mineral. Geochemistry* **54**, 115–149.

Fietzke J., Ragazzola F., Halfar J., Dietze H., Foster L. C., Hansteen T. H., Eisenhauer A. and Steneck R. S. (2015) Century-scale trends and seasonality in pH and temperature for shallow zones of the Bering Sea. *Proc. Natl. Acad. Sci.* **112**, 2960–2965.

Foster G. L. (2008) Seawater pH, pCO2 and [CO3]2- variations in the Caribbean Sea over the last 130 kyr: A boron isotope and B/Ca study of planktic foraminifera. *Earth Planet. Sci. Lett.* **271**, 254–266.

Foster G. L., Hönisch B., Paris G., Dwyer G. S., Rae J. W. B., Elliott T., Gaillardet J., Hemming N. G., Louvat P. and Vengosh A. (2013) Interlaboratory comparison of boron isotope analyses of boric acid, seawater and marine CaCO3 by MC-ICPMS and NTIMS. *Chem. Geol.* **358**, 1–14.

Foster G. L., Pogge von Strandmann P. A. E. and Rae J. W. B. (2010) Boron and magnesium isotopic composition of seawater. *Geochemistry, Geophys. Geosystems* **11**, 1–10.

Foster G. L. and Rae J. W. B. (2016) Reconstructing Ocean pH with Boron Isotopes in Foraminifera. *Annu. Rev. Earth Planet. Sci.* **44**, 207–237.

Gabitov R. I., Rollion-Bard C., Tripati A. and Sadekov A. (2014) In situ study of boron partitioning between calcite and fluid at different crystal growth rates. *Geochim. Cosmochim. Acta* **137**, 81–92.

Gaetani G. A. and Cohen A. L. (2006) Element partitioning during precipitation of aragonite from seawater: A framework for understanding paleoproxies. *Geochim. Cosmochim. Acta* **70**, 4617–4634.

Gagnon A. C., Adkins J. F. and Erez J. (2012) Seawater transport during coral biomineralization. *Earth Planet. Sci. Lett.* **329–330**, 150–161.

Gagnon A. C., Adkins J. F., Fernandez D. P. and Robinson L. F. (2007) Sr/Ca and Mg/Ca vital effects correlated with skeletal architecture in a scleractinian deep-sea coral and the role of Rayleigh fractionation. *Earth Planet. Sci. Lett.* **261**, 280–295.

Gaillardet J. and Allègre C. J. (1995) Boron isotopic compositions of corals: Seawater or diagenesis record? *EPSL* **136**, 665–676.

Gao K., Aruga Y., Asada K., Ishihara T., Akano T. and Kiyohara M. (1993) Calcification in the articulated coralline alga *Corallina pilulifera*, with special reference to the effect of elevated CO2 concentration. *Mar. Biol.* **117**, 129–132.

Gao K. and Zheng Y. (2009) Combined effects of ocean acidification and solar UV radiation on photosynthesis, growth, pigmentation and calcification of the coralline alga *Corallina sessilis* (*Rhodophyta*). *Glob. Chang. Biol.* **16**, 2388–2398.

Gattuso J.-P., Magnan A., Bille R., Cheung W. W. L., Howes E. L., Joos F., Allemand D., Bopp L., Cooley S. R., Eakin C. M., Hoegh-Guldberg O., Kelly R. P., Portner H.-O., Rogers a. D., Baxter J. M., Laffoley D., Osborn D., Rankovic A., Rochette J., Sumaila U. R., Treyer S. and Turley C. (2015) Contrasting futures

for ocean and society from different anthropogenic CO2 emissions scenarios. *Science (80-.).* **349**, aac4722-1-aac4722-10.

Gattuso J. P., Frankignoulle M., Bourge I., Romaine S. and Buddemeier R. W. (1998) Effect of calcium carbonate saturation of seawater on coral calcification. *Glob. Planet. Change* **18**, 37–46.

Hall-Spencer J. M., Rodolfo-Metalpa R., Martin S., Ransome E., Fine M., Turner S. M., Rowley S. J., Tedesco D. and Buia M.-C. (2008) Volcanic carbon dioxide vents show ecosystem effects of ocean acidification. *Nature* **454**, 96–99.

Hemming N. G. and Hanson G. N. (1992) Boron isotopic composition and concentration in modern marine carbonates. *Geochim. Cosmochim. Acta* **56**, 537–543.

Hemming N. G., Reeder R. J. and Hart S. R. (1998) Growth-step-selective incorporation of boron on the calcite surface. *Geochim. Cosmochim. Acta* **62**, 2915–2922.

Henehan M. J., Foster G. L., Rae J. W. B., Prentice K. C., Erez J., Bostock H. C., Marshall B. J. and Wilson P. A. (2015) Evaluating the utility of B/Ca ratios in planktic foraminifera as a proxy for the carbonate system: A case study of *Globigerinoides ruber*. *Geochemistry, Geophys. Geosystems*, 1052–1069.

Henehan M. J., Rae J. W. B., Foster G. L., Erez J., Prentice K. C., Kucera M., Bostock H. C., Martínez-Botí M. a., Milton J. A., Wilson P. a., Marshall B. J. and Elliott T. (2013) Calibration of the boron isotope proxy in the planktonic foraminifera *Globigerinoides ruber* for use in palaeo-CO2 reconstruction. *Earth Planet. Sci. Lett.* **364**, 111–122.

Holcomb M., Venn A. A., Tambutté E., Tambutté S., Allemand D., Trotter J. and McCulloch M. (2014) Coral calcifying fluid pH dictates response to ocean acidification. *Sci. Rep.* **4**, 1–4.

Hönisch B., Hemming N. G., Grottoli A. G., Amat A., Hanson G. N. and Bijma J. (2004) Assessing scleractinian corals as recorders for paleo-pH: Empirical calibration and vital effects. *Geochim. Cosmochim. Acta* **68**, 3675–3685.

Hurd C. L., Cornwall C. E., Currie K., Hepburn C. D., McGraw C. M., Hunter K. A. and Boyd P. W. (2011) Metabolically induced pH fluctuations by some coastal calcifiers exceed projected 22nd century ocean acidification: a mechanism for differential susceptibility? *Glob. Chang. Biol.* **17**, 3254–3262.

Kamenos N. A., Perna G., Gambi M. C., Micheli F. and Kroeker K. J. (2016) Coralline algae in a naturally acidified ecosystem persist by maintaining control of skeletal mineralogy and size. *Proc. R. Soc. B* **283**, 20161159.

Keul N., Langer G., Thoms S., de Nooijer L. J., Reichart G. J. and Bijma J. (2017) Exploring foraminiferal Sr/Ca as a new carbonate system proxy. *Geochim. Cosmochim. Acta* **202**, 374–386.

Klochko K., Kaufman A. J., Yao W., Byrne R. H. and Tossell J. A. (2006) Experimental measurement of boron isotope fractionation in seawater. *Earth Planet. Sci. Lett.* **248**, 276–285.

Krief S., Hendy E. J., Fine M., Yam R., Meibom A., Foster G. L. and Shemesh A. (2010) Physiological and isotopic responses of scleractinian corals to ocean acidification. *Geochim. Cosmochim. Acta* **74**, 4988–5001.

Kuffner I. B., Andersson A. J., Jokiel P. L., Rodgers K. S. and Mackenzie F. T. (2008) Decreased abundance of crustose coralline algae due to ocean acidification. *Nat. Geosci.* **1**, 114–117.

Mackinder L., Wheeler G., Schroeder D., Riebesell U. and Brownlee C. (2010) Molecular Mechanisms Underlying Calcification in Coccolithophores. *Geomicrobiol. J.* **27**, 585–595.

Martin S., Charnoz A. and Gattuso J.-P. (2013) Photosynthesis, respiration and calcification in the Mediterranean crustose coralline alga *Lithophyllum cabiochae* (*Corallinales, Rhodophyta*). *Eur. J. Phycol.* **48**, 163–172.

Martin S. and Gattuso J.-P. (2009) Response of Mediterranean coralline algae to ocean acidification and elevated temperature. *Glob. Chang. Biol.* **15**, 2089–2100.

Mavromatis V., Montouillout V., Noireaux J., Gaillardet J. and Schott J. (2015) Characterization of boron incorporation and speciation in calcite and aragonite from co-precipitation experiments under controlled pH, temperature and precipitation rate. *Geochim. Cosmochim. Acta* **150**, 299–313.

McConnaughey T. A. and Falk R. H. (1991) Calcium-proton exchange during algal calcification. *Biol. Bull.* **180**, 185–195.

McCoy S. J. and Kamenos N. A. (2015) Coralline algae (*Rhodophyta*) in a changing world: integrating ecological, physiological, and geochemical responses to global change. *J. Phycol.* **51**, 6–24.

McCulloch M., Falter J., Trotter J. and Montagna P. (2012) Coral resilience to ocean acidification and global warming through pH up-regulation. *Nat. Clim. Chang.* **2**, 623–627.

McCulloch M., Trotter J., Montagna P., Falter J., Dunbar R., Freiwald A., Försterra G., López Correa M., Maier C., Rüggeberg A. and Taviani M. (2012) Resilience of cold-water scleractinian corals to ocean acidification: Boron isotopic systematics of pH and saturation state up-regulation. *Geochim. Cosmochim. Acta* **87**, 21–34.

Mucci A. (1983) The solubility of calcite and aragonite in seawater at various salinities, temperatures and one atmosphere total pressure. *Am. J. Sci.* **283**, 780–799.

Nir O., Vengosh A., Harkness J. S., Dwyer G. S. and Lahav O. (2015) Direct measurement of the boron isotope fractionation factor: Reducing the uncertainty in reconstructing ocean paleo-pH. *Earth Planet. Sci. Lett.* **414**, 1–5.

Noireaux J., Mavromatis V., Gaillardet J., Schott J., Montouillout V., Louvat P., Rollion-Bard C. and Neuville D. R. (2015) Crystallographic control on the boron isotope paleo-pH proxy. *Earth Planet. Sci. Lett.* **430**, 398–407.

de Nooijer L. J., Spero H. J., Erez J., Bijma J. and Reichart G. J. (2014) Biomineralization in perforate foraminifera. *Earth-Science Rev.* **135**, 48–58.

Palmer M. R. (1998) Reconstructing Past Ocean pH-Depth Profiles. *Science (80-.).* **282**, 1468–1471.

Pauly M., Kamenos N. A., Donohue P. and LeDrew E. (2015) Coralline algal Mg-O bond strength as a marine pCO2 proxy. *Geology* **43**, 267–270.

Rae J. W. B., Foster G. L., Schmidt D. N. and Elliott T. (2011) Boron isotopes and B/Ca in benthic foraminifera: Proxies for the deep ocean carbonate system. *Earth Planet. Sci. Lett.* **302**, 403–413.

Ragazzola F., Foster L. C., Form A., Anderson P. S. L., Hansteen T. H. and Fietzke J. (2012) Ocean acidification weakens the structural integrity of coralline algae. *Glob. Chang. Biol.* **18**, 2804–2812.

Reynaud S., Hemming N. G., Juillet-Leclerc A. and Gattuso J. P. (2004) Effect of pCO2 and temperature on the boron isotopic composition of the zooxanthellate coral *Acropora* sp. *Coral Reefs* **23**, 539–546.

Riebesell U., Zondervan I., Rost B., Tortell P. D., Zeebe R. E. and Morel F. M. (2000) Reduced calcification of marine plankton in response to increased atmospheric CO2. *Nature* **407**, 364–7.

Ries J. B. (2011a) A physicochemical framework for interpreting the biological calcification response to CO2-induced ocean acidification. *Geochim. Cosmochim. Acta* **75**, 4053–4064.

Ries J. B. (2009) Effects of secular variation in seawater Mg/Ca ratio (calcite-aragonite seas) on CaCO3 sediment production by the calcareous algae *Halimeda, Penicillus* and *Udotea* - Evidence from recent experiments and the geological record. *Terra Nov.* **21**, 323–339.

Ries J. B. (2011b) Skeletal mineralogy in a high-CO2 world. *J. Exp. Mar. Bio. Ecol.* **403**, 54–64.

Ries J. B., Cohen A. L. and McCorkle D. C. (2009) Marine calcifiers exhibit mixed responses to CO2-induced ocean acidification. *Geology* **37**, 1131–1134.

Ries J. B., Ghazaleh M. N., Connolly B., Westfield I. and Castillo K. D. (2016) Impacts of seawater saturation state and temperature on the dissolution kinetics of whole-shell biogenic carbonates. *Geochim. Cosmochim. Acta* **192**, 318–337.

Roleda M. Y., Cornwall C. E., Feng Y., McGraw C. M., Smith A. M. and Hurd C. L. (2015) Effect of Ocean Acidification and pH Fluctuations on the Growth and Development of Coralline Algal Recruits, and an Associated Benthic Algal Assemblage. *PLoS One* **10**, e0140394.

Rollion-Bard C., Blamart D., Trebosc J., Tricot G., Mussi A. and Cuif J. P. (2011) Boron isotopes as pH proxy: A new look at boron speciation in deep-sea corals using 11B MAS NMR and EELS. *Geochim.*

Cosmochim. Acta **75**, 1003–1012.

Rollion-Bard C., Chaussidon M. and France-Lanord C. (2003) pH control on oxygen isotopic composition of symbiotic corals. *Earth Planet. Sci. Lett.* **215**, 275–288.

Roy R. N., Roy L. N., Vogel K. M., Portermoore C., Pearson T., Good C. E., Millero F. J. and Campbell D. M. (1993) The dissociation constants of carbonic acid in seawater at salinities 5 to 45 and temperatures 0 degrees C to 45 degrees C. *Mar. Chem.* **44**, 249–267.

Sanyal a, Hemming N. G., Broecker W. S., Lea D. W., Spero H. J. and Hanson G. N. (1996) Oceanic pH control on the boron isotopic composition of foraminifera: Evidence from culture experiments. *Paleoceanography* **11**, 513–517.

Semesi I. S., Kangwe J. and Björk M. (2009) Alterations in seawater pH and CO2 affect calcification and photosynthesis in the tropical coralline alga, *Hydrolithon* sp. (*Rhodophyta*). *Estuar. Coast. Shelf Sci.* **84**, 337–341.

Smith A. D. and Roth A. A. (1979) Effect of carbon dioxide concentration on calcification in the red coralline alga *Bossiella orbigniana*. *Mar. Biol.* **52**, 217–225.

Spivack A. J., You C.-F. and Smith H. J. (1993) Foraminiferal boron isotope ratios as a proxy for surface ocean pH over the past 21 Myr. *Nature* **363**, 149–151.

Stewart J. A., Anagnostou E. and Foster G. L. (2016) An improved boron isotope pH proxy calibration for the deep-sea coral *Desmophyllum dianthus* through sub-sampling of fibrous aragonite. *Chem. Geol.* **447**, 148–160.

Stoll H., Langer G., Shimizu N. and Kanamaru K. (2012) B/Ca in coccoliths and relationship to calcification vesicle pH and dissolved inorganic carbon concentrations. *Geochim. Cosmochim. Acta* **80**, 143–157.

Tans P. (NOAA/ESRL) and Keeling R. (Scripps I. of O. (2016) ESRL Global Monitoring Division.

Trotter J., Montagna P., McCulloch M., Silenzi S., Reynaud S., Mortimer G., Martin S., Ferrier-Pagès C., Gattuso J. P. and Rodolfo-Metalpa R. (2011) Quantifying the pH "vital effect" in the temperate zooxanthellate coral *Cladocora caespitosa*: Validation of the boron seawater pH proxy. *Earth Planet. Sci. Lett.* **303**, 163–173.

Uchikawa J., Penman D. E., Zachos J. C. and Zeebe R. E. (2015) Experimental evidence for kinetic effects on B/Ca in synthetic calcite: Implications for potential B(OH)4− and B(OH)3 incorporation. *Geochim. Cosmochim. Acta* **150**, 171–191.

Vengosh A., Kolodny Y., Starinsky A., Chivas A. R. and McCulloch M. T. (1991) Coprecipitation and isotopic fractionation of boron in modern biogenic carbonates. *Geochim. Cosmochim. Acta* **55**, 2901–2910.

Venn A. A., Tambutté E., Holcomb M., Laurent J., Allemand D. and Tambutté S. (2013) Impact of seawater acidification on pH at the tissue–skeleton interface and calcification in reef corals. *Proc. Natl. Acad. Sci.* **110**, 1634–1639.

Venn A., Tambutté E., Holcomb M., Allemand D. and Tambutté S. (2011) Live tissue imaging shows reef corals elevate pH under their calcifying tissue relative to seawater. *PLoS One* **6**, e20013.

Yu J., Elderfield H. and Hönisch B. (2007) B/Ca in planktonic foraminifera as a proxy for surface seawater pH. *Paleoceanography* **22**, PA2202.

Zeebe R. E. and Wolf-Gladrow D. (2001) *CO2 in Seawater: Equilibrium, Kinetics, Isotopes*. Third., Elsevier Ltd, Oxford.

Figure captions

Figure 1. Calcification rates of coralline red algae plotted against pH_{sw}. Comparison between calcification trends in coralline red algae descried in Smith and Roth (1979; *Bossiella orbigniana*) (**A**) and Ries *et al*. (2009; *Neogoniolithon* sp.) (**B**). Although calcification rates are reported in different units, both studies suggest that coralline algae exhibit a parabolic calcification response to CO_2-induced ocean acidification, with an optimum near pH_{sw} 7.9.

Figure 2. $\delta^{11}B$ of the coralline red algae *Neogoniolithon* sp. measured using MC-ICPMS, plotted against pH_{sw}. Black circles filled with grey represent replicates measured at each pH_{sw}, and the mean $\delta^{11}B$ of each culture experiment is shown as a filled black circle. The $\delta^{11}B$ of all measured samples are elevated relative to aqueous borate (blue line) by +12 ‰ on average. $\delta^{11}B$ compositions of a crustose species of *Neogoniolithon* coralline red alga and various scleractinian corals grown at different pH_{sw} are plotted in open coloured symbols (Cornwall et al., 2017; Honisch et al., 2004; Reynaud et al., 2004; Krief et al., 2010; Anagnostou et al., 2012; McCulloch et al., 2012a; Holcomb et al., 2014).

Figure 3. Least squares linear regression of B/Ca and Sr/Ca against $\delta^{11}B$ composition. (**A**) B/Ca ratios in *Neogoniolithon* sp. show a strong positive correlation when regressed against $\delta^{11}B$ composition. (**B**) Sr/Ca ratios show slightly less well-defined trends when regressed against $\delta^{11}B$ composition, although both reveal statistically significant correlations.

Figure 4. pH_{cf} *vs*. pH_{sw} (A) and ΔpH ($pH_{cf} - pH_{sw}$) *vs*. pH_{sw} (B). An apparent parabolic relationship is observed in **A**, with a maximum at pH_{cf} ~7.95. In **B**, ΔpH also exhibits a similar relationship with pH_{sw} suggesting that coralline red algae increase their pH_{cf} by increasingly larger amounts under acidified conditions to support biogenic calcification. At extremely low pH_{sw}, the shape of the curve suggests that coralline red algae have reached the limit of the extent to which they can elevate pH_{cf} relative to pH_{sw}. The filled black circles indicate mean values. This branching species of *Neogoniolithon* coralline red algae is compared with a crustose species of *Neogoniolithon* (stars) from Cornwall et al. (2017).

Figure 5. B/Ca and Sr/Ca regressed against pH_{sw}. Sr/Ca ratios (**A**) of *Neogoniolithon* sp. are strongly linearly correlated with pH_{sw}, while B/Ca is strongly correlated with an apparent parabolic relationship with pH_{sw} (**B**). Sr/Ca (**C**) is not significantly correlated with B/Ca, although the trend is nearly significant. The filled black circles indicate mean values.

Figure 6. The relationship between the pH_{cf} and net calcification of *Neogoniolithon* sp. (**A**) This positive correlation between the mean pH_{cf} and mean calcification rate indicates a reduction in calcification rate with decreasing pH_{cf}. (**B**) Across treatments, pH_{cf} (black circles) is influenced by pH_{sw}, which also affects net calcification (red squares). The similarity between the two negative curves highlights the link between calcification rate and pH_{sw}, but also reveals the resilience of coralline red algae to moderate ocean acidification. The algae are able to mitigate moderate pH_{sw} reduction, but are unable to calcify efficiently at extremely low pH_{sw} values.

Table captions

Table 1. Summary of each experimental treatment showing measured element ratios and $\delta^{11}B$ composition. The mean of each variable measured is shown in bold, 1σ are shown in parentheses. The sample shown in red is anomalous and is therefore excluded from subsequent discussion (also excluded from means). Therefore n = 16 for all regression analyses.

Table 2. Mean skeletal $\delta^{11}B$ compositions for each experimental treatment, along with percentage of boric acid (enriched in ^{11}B by 27.2 ‰) required to be incorporated into the algal calcite to generate the measured $\delta^{11}B$ composition, assuming that $\delta^{11}B$ of the borate portion of the algal calcite is equal to seawater borate. Net calcification indicates that algae from the pH_{sw} 8.19 and 7.49 treatments have the slowest calcification rates, yet also require the smallest apparent proportion of boric acid. pH_{cf} indicates mean calcification site pH for each treatment, and ΔpH describes the change in pH according to the equation $\Delta pH = pH_{cf} - pH_{sw}$. 1σ are shown in parentheses.

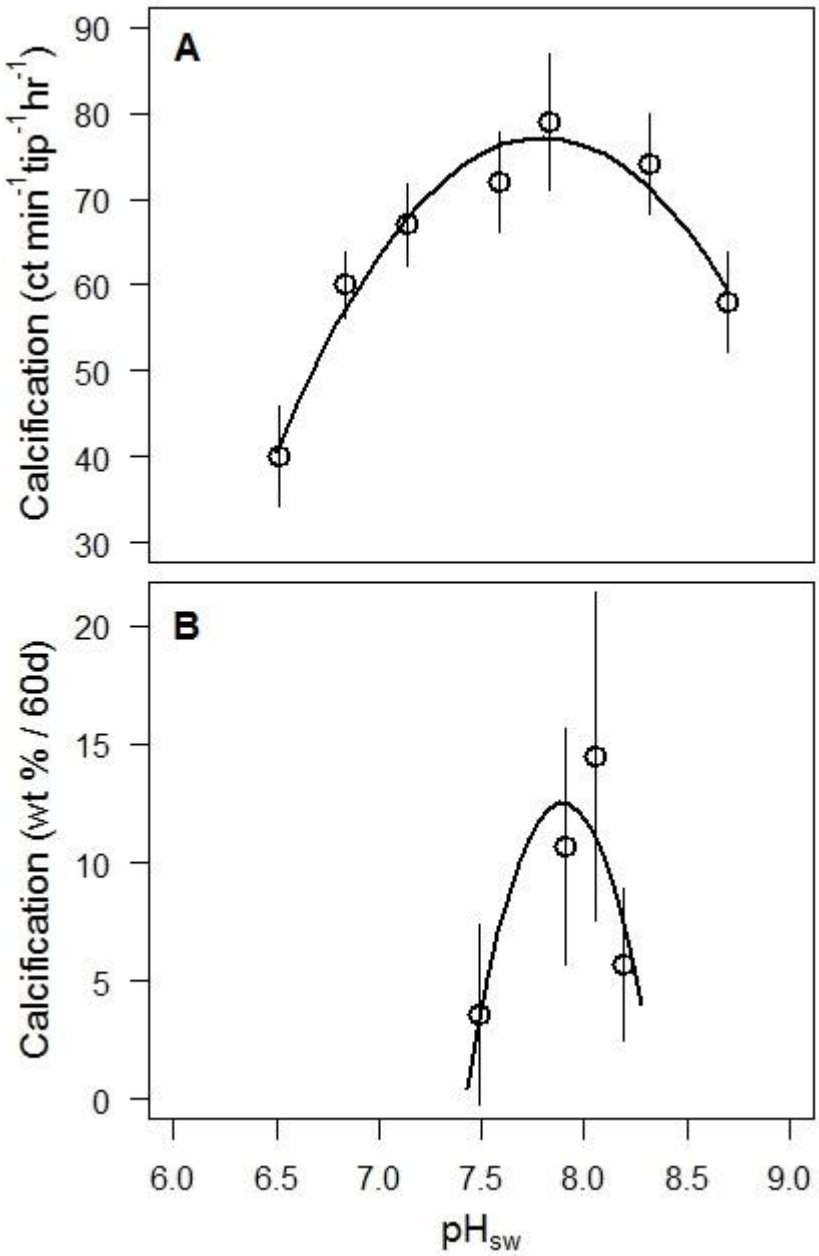
A
B
Calcification (ct min-1tip-1hr-1)
Calcification (wt % / 60d)
pHsw
90
80
70
60
50
40
30
20
15
10
5
0
6.0
6.5
7.0
7.5
8.0
8.5
9.0

791

792

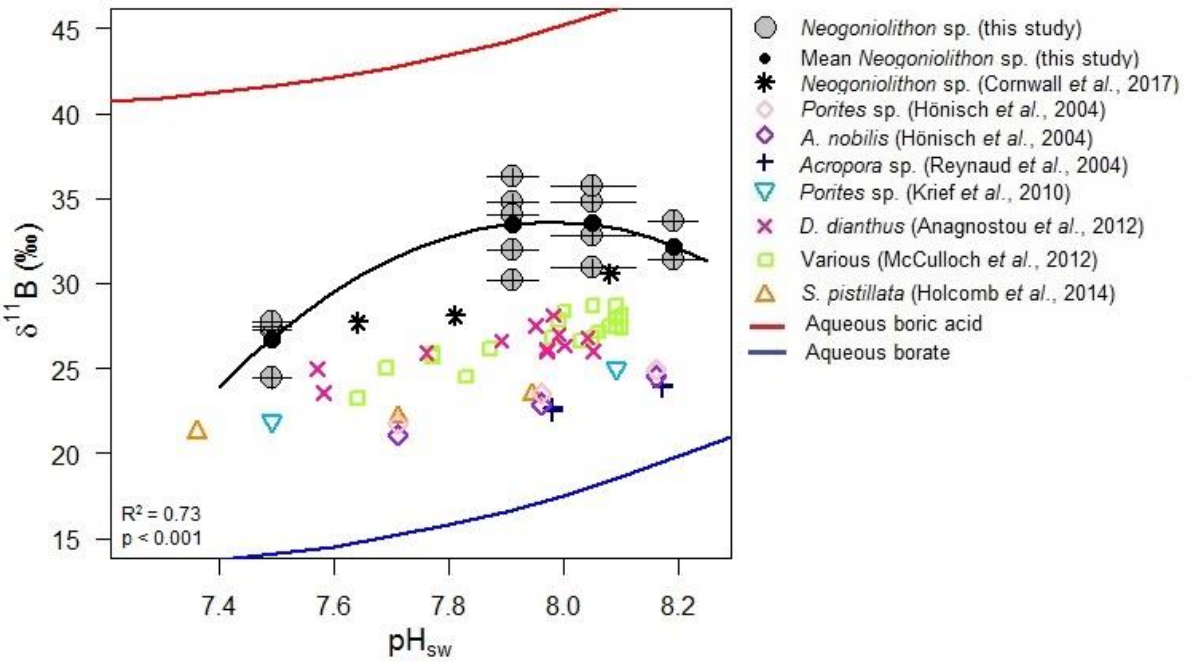
45
40
35
30
25
20
15
$\delta^{11}B$ (‰)
7.4
7.6
7.8
8.0
8.2
pH_{sw}
$R^2 = 0.73$
$p < 0.001$
Neogoniolithon sp. (this study)
Mean *Neogoniolithon* sp. (this study)
Neogoniolithon sp. (Cornwall *et al.*, 2017)
Porites sp. (Hönisch *et al.*, 2004)
A. nobilis (Hönisch *et al.*, 2004)
Acropora sp. (Reynaud *et al.*, 2004)
Porites sp. (Krief *et al.*, 2010)
D. dianthus (Anagnostou *et al.*, 2012)
Various (McCulloch *et al.*, 2012)
S. pistillata (Holcomb *et al.*, 2014)
Aqueous boric acid
Aqueous borate

793

794

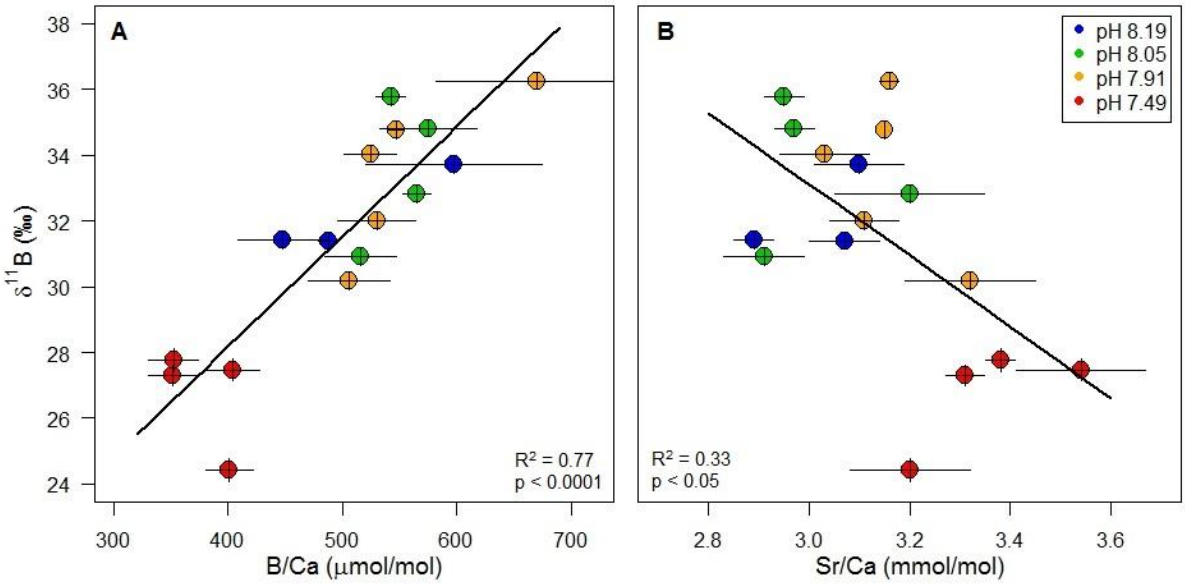
A
B
pH 8.19
pH 8.05
pH 7.91
pH 7.49
$R^2 = 0.77$
$p < 0.0001$
$R^2 = 0.33$
$p < 0.05$
$\delta^{11}B$ (‰)
B/Ca (μmol/mol)
Sr/Ca (mmol/mol)
38
36
34
32
30
28
26
24
300
400
500
600
700
2.8
3.0
3.2
3.4
3.6

795

796

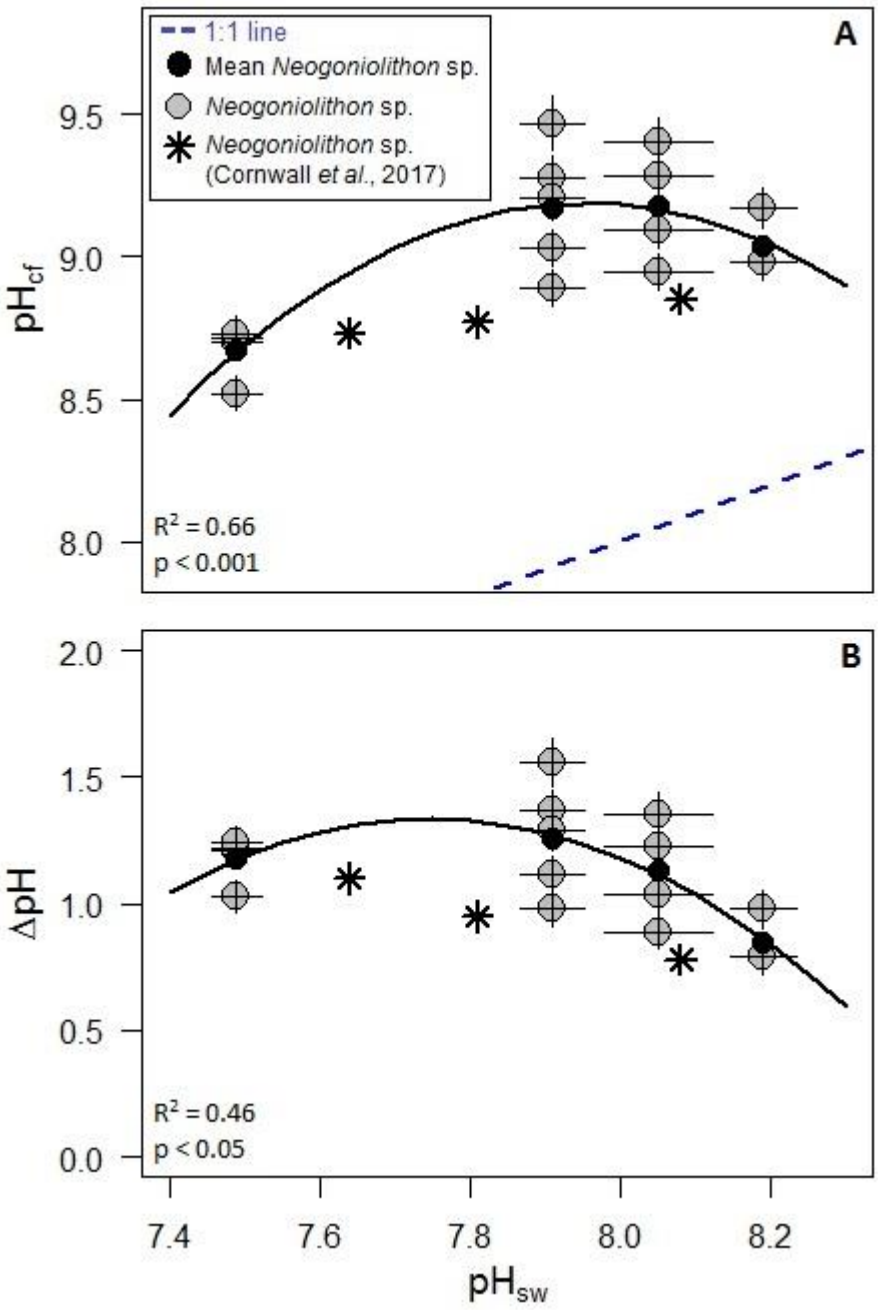
1:1 line
Mean Neogoniolithon sp.
Neogoniolithon sp.
Neogoniolithon sp.
(Cornwall et al., 2017)
A
B
pHcf
ΔpH
pHsw
R² = 0.66
p < 0.001
R² = 0.46
p < 0.05
9.5
9.0
8.5
8.0
2.0
1.5
1.0
0.5
0.0
7.4
7.6
7.8
8.0
8.2

797

798

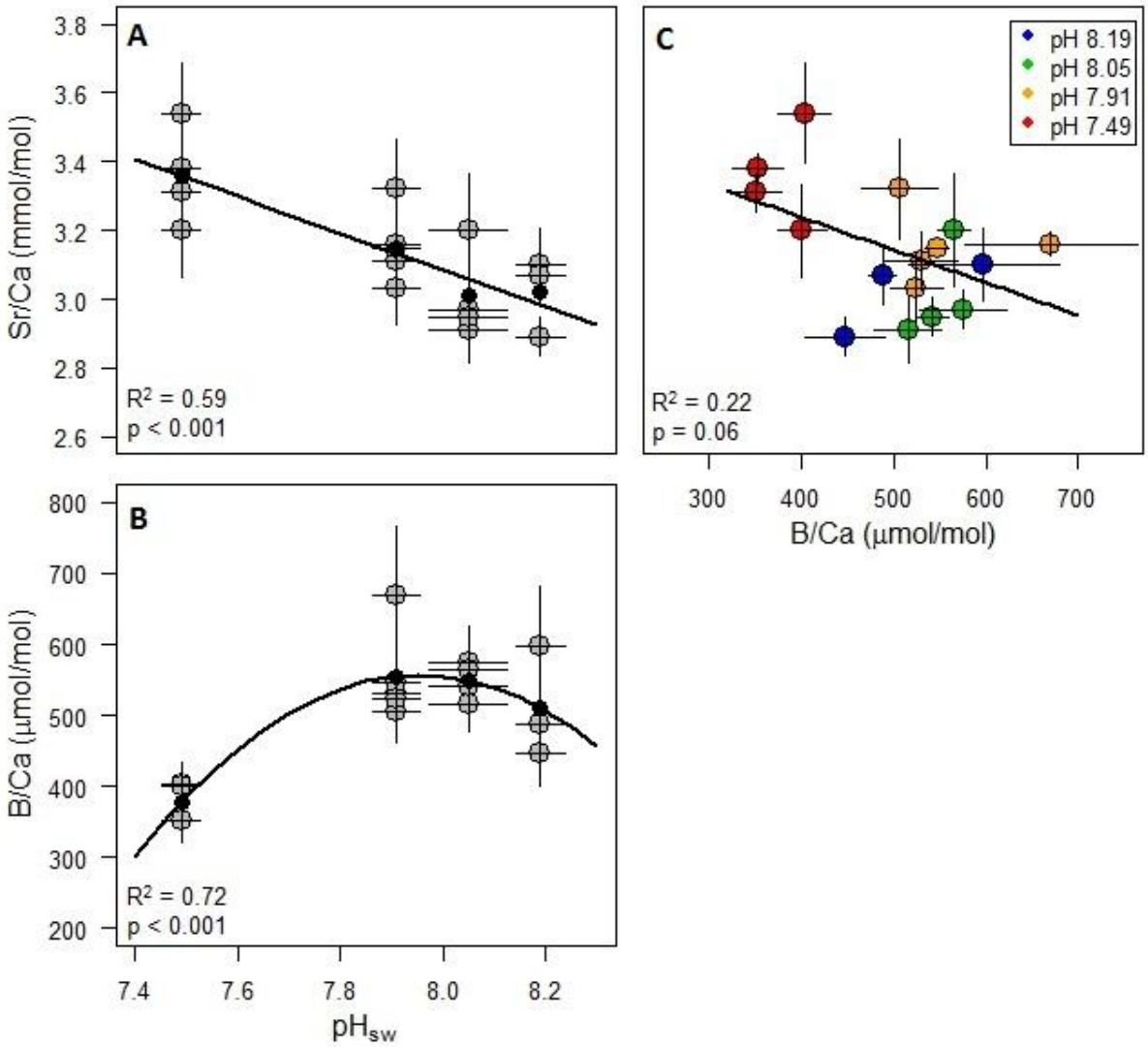
A
Sr/Ca (mmol/mol)
3.8
3.6
3.4
3.2
3.0
2.8
2.6
R² = 0.59
p < 0.001
C
pH 8.19
pH 8.05
pH 7.91
pH 7.49
R² = 0.22
p = 0.06
300
400
500
600
700
B/Ca (µmol/mol)
B
B/Ca (µmol/mol)
800
700
600
500
400
300
200
R² = 0.72
p < 0.001
7.4
7.6
7.8
8.0
8.2
pHsw

799

800

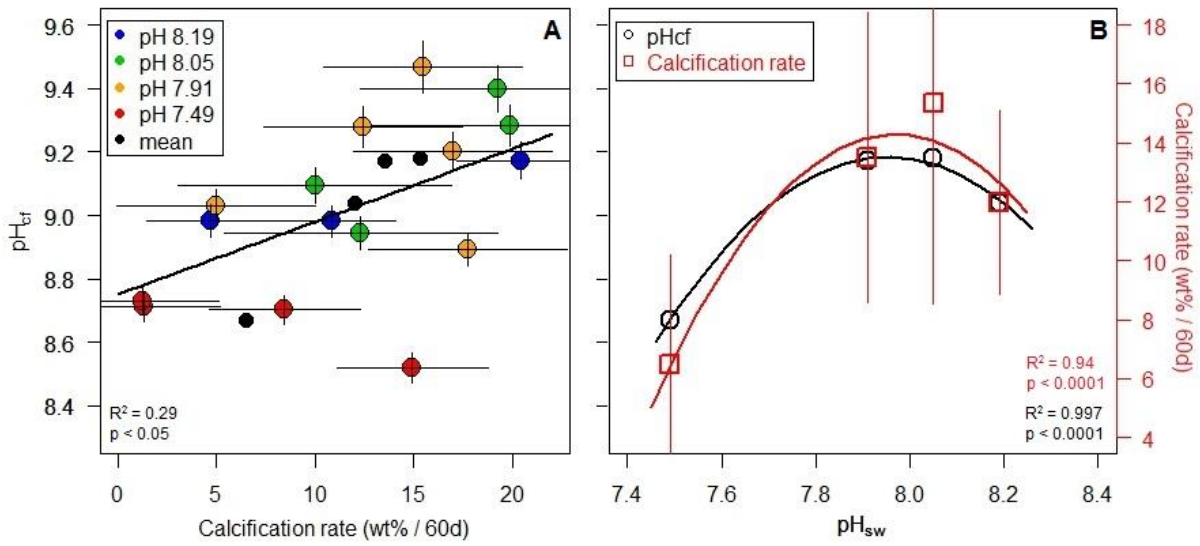
A
pH 8.19
pH 8.05
pH 7.91
pH 7.49
mean
$R^2 = 0.29$
$p < 0.05$
pH_{cf}
Calcification rate (wt% / 60d)
B
pHcf
Calcification rate
$R^2 = 0.94$
$p < 0.0001$
$R^2 = 0.997$
$p < 0.0001$
pH_{sw}
Calcification rate (wt% / 60d)

Table 1.

pCO_2	pH	$\delta^{11}B$ ‰				B/Ca µmol mol^{-1}				^{11}B nmol				Sr/Ca n	
µatm		Replicate	Duplicate	Average	Experiment mean	Replicate	Duplicate	Average	Experiment mean	Replicate	Duplicate	Average	Experiment mean	Replicate	Duplicate
		40.61 (0.10)	*39.18 (0.11)*	*39.90*		*815 (41)*	*686 (34)*	*751*		*800 (132)*	*533 (57)*	*667*		*2.89 (0.14)*	*2.99 (0.15)*
409 (6)	8.19 (0.03)	31.44 (0.13)	31.38 (0.11)	**31.41**	**32.17 (1.33)**	454 (29)	439 (39)	**447**	**511 (78)**	354 (84)	415 (40)	**395**	**415 (62)**	2.85 (0.10)	2.93 (0.04)
		33.70 (0.11)				**598 (73)**				**590 (83)**				**3.10 (0.08)**	
		31.40 (0.12)				**488 (5)**				**530 (41)**				**3.07 (0.06)**	
		35.02 (0.10)	34.60 (0.11)	**34.81**		628 (52)	521 (24)	**575**		545 (24)	440 (50)	**493**		2.99 (0.01)	2.95 (0.04)
606 (7)	8.05 (0.06)	**30.90 (0.10)**			**33.58 (2.16)**	**516 (27)**			**550 (26)**	**466 (32)**			**516 (36)**	**2.91 (0.07)**	
		32.83 (0.14)				**565 (8)**				**500 (8)**				**3.20 (0.14)**	
		35.77 (0.11)				**542 (9)**				**603 (65)**				**2.95 (0.03)**	
		32.05 (0.16)	31.99 (0.10)	**32.02**		488 (44)	572 (15)	**530**		452 (18)	513 (25)	**483**		3.02 (0.09)	3.19 (0.03)
		34.75 (0.11)				**547 (3)**				**371 (75)**				**3.15 (0.00)**	
903 (12)	7.91 (0.03)	**30.18 (0.15)**			**33.45 (2.38)**	**506 (32)**			**555 (66)**	**488 (7)**			**477 (49)**	**3.32 (0.12)**	
		36.26 (0.10)				**670 (84)**				**641 (115)**				**3.16 (0.01)**	
		34.03 (0.10)				**524 (19)**				**401 (54)**				**3.03 (0.08)**	
		27.31 (0.18)				**352 (18)**				**69 (66)**				**3.31 (0.03)**	
2856 (54)	7.49 (0.02)	**27.47 (0.18)**			**26.75 (1.56)**	**404 (19)**			**377 (29)**	**373 (149)**			**163 (74)**	**3.54 (0.13)**	
		27.78 (0.21)				**352 (18)**				**100 (44)**				**3.38 (0.02)**	
		24.42 (0.22)				**401 (17)**				**108 (39)**				**3.20 (0.11)**	

803

Table 2.

pCO_2	pH_{sw}	$\delta^{11}B$	$B(OH)_3$	Net calcification	pH_{cf}	ΔpH
µatm		‰	%	wt% / 60 days		
409 (6)	8.19 (0.03)	32.17 (1.33)	44 (4)	5.7 (2.9)	9.04 (0.11)	0.85 (0.11)
606 (7)	8.05 (0.06)	33.58 (2.16)	57 (7)	14.5 (6.6)	9.18 (0.20)	1.13 (0.20)
903 (12)	7.91 (0.03)	33.45 (2.38)	60 (8)	10.7 (4.7)	9.17 (0.22)	1.26 (0.22)
2856 (54)	7.49 (0.02)	26.75 (1.56)	46 (6)	3.6 (3.5)	8.67 (0.10)	1.18 (0.10)

Supplementary material

Table captions

Table SM1. Further details of the culture experiment from Ries et al. (2009). Values for all tanks as well as individual culture treatment tanks are shown with ± 1σ.

Table SM2. Statistical analysis of all parameters investigated in this study. Regressions, regression equations and significance values are all described in further detail.

Figure captions

Figure SM1. Sr/Ca *vs.* DIC (A), B/Ca *vs.* DIC (B), and B/Ca *vs.* net calcification (C). These relationships were explored further following a recent paper investigating foraminiferal Sr/Ca as a new carbonate system proxy (Keul et al., 2017). With an enhanced DIC influx, Ω increases, and therefore Ca influx decreases, hence a positive relationship can be found between DIC and Sr/Ca. Net calcification appears to have a dominant role in determining B/Ca, as opposed to DIC determining Sr/Ca. B/Ca ratios have a strong positive correlation with net calcification, and whilst there is a negative relationship present between B/Ca and DIC, this is most likely due to typically lower calcification rates at higher DIC.

Figure SM2. Size of sample plotted against difference from mean $\delta^{11}B$. This relationship reveals there are comparable ranges of difference between the measured $\delta^{11}B$ and the mean $\delta^{11}B$ for every pH_{sw} treatment, no matter the size of sample measured. This indicates there is no bias towards larger samples, and that $\delta^{11}B$ is unaffected by the size of the initial sample.

References

Mucci A. (1983) The solubility of calcite and aragonite in seawater at various salinities, temperatures and one atmosphere total pressure. *Am. J. Sci.* **283**, 780–799.

Ries J. B., Cohen A. L. and McCorkle D. C. (2009) Marine calcifiers exhibit mixed responses to CO2-induced ocean acidification. *Geology* **37**, 1131–1134.

Roy R. N., Roy L. N., Vogel K. M., Portermoore C., Pearson T., Good C. E., Millero F. J. and Campbell D. M. (1993) The dissociation constants of carbonic acid in seawater at salinities 5 to 45 and temperatures 0 degrees C to 45 degrees C. *Mar. Chem.* **44**, 249–267.

Table SM1.

	All	pH 8.19	pH 8.05	pH 7.91	pH 7.49
Sample location	Atlantic Ocean, FL				
Number of tanks	4				
Filter rate (L/h)	600				
Irradiance (W/m²)	426				
K_{sp}	(Mucci, 1983)				
K_1 and K_2	(Roy et al., 1993)				
Water temperature (°C)		25.0 ± 0.055	25.0 ± 0.152	25.1 ± 0.164	24.9 ± 0.130
Salinity (psu)		31.8 ± 0.207	31.7 ± 0.118	31.5 ± 0.155	31.8 ± 0.258
Ω_{arag}		3.12 ± 0.221	2.40 ± 0.420	1.84 ± 0.129	0.90 ± 0.050
DIC		1738 ± 50.35	1786 ± 100.71	1903 ± 45.91	2350 ± 33.21

Table SM2.

Parameter 1	Parameter 2	Regression	Equation	R^2	p
$\delta^{11}B$	pH_{sw}	Curve	$y = -30x^2 + 472x - 1846$	0.73	< 0.001
$\delta^{11}B$	B/Ca	Linear	$y = 0.034x + 14.8$	0.77	< 0.0001
$\delta^{11}B$	Sr/Ca	Linear	$y = -10.8x + 65.6$	0.33	< 0.05
pH_{cf}	pH_{sw}	Curve	$y = -2.4x^2 + 38.5x - 143.8$	0.66	< 0.001
ΔpH	pH_{sw}	Curve	$y = -2.4x^2 + 37.6x - 144.3$	0.46	< 0.05
Sr/Ca	pH_{sw}	Linear	$y = -0.53x + 7.3$	0.59	< 0.001
B/Ca	pH_{sw}	Curve	$y = -833x^2 + 13258x - 52173$	0.72	< 0.001
Sr/Ca	B/Ca	Linear	$y = -0.001x + 3.6$	0.22	0.06
pH_{cf}	Calcification rate	Linear	$y = 0.023x + 8.8$	0.29	< 0.05
Calcification rate	pH_{sw}	Curve	$y = -34x^2 + 545x - 2161$	0.94	< 0.0001

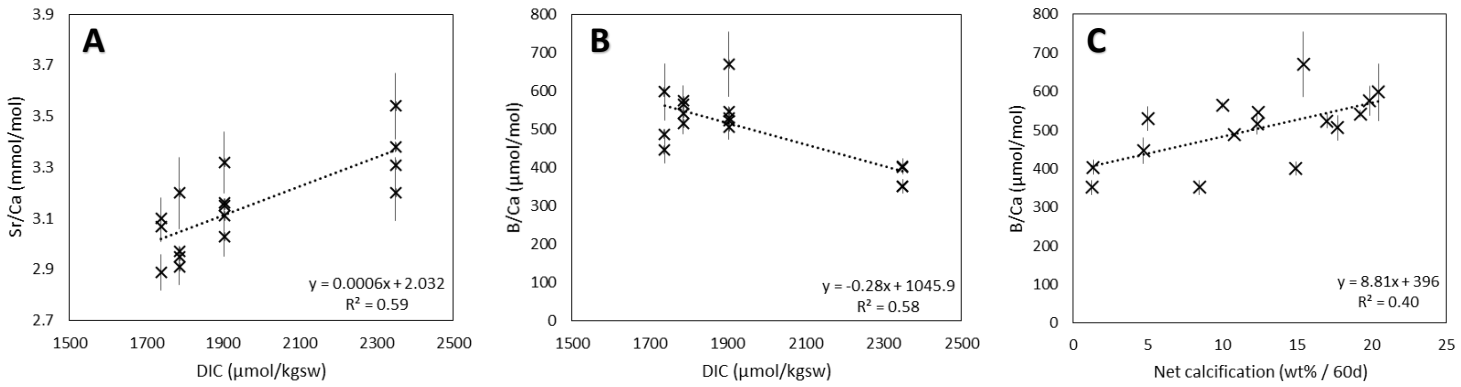
A
Sr/Ca (mmol/mol)
DIC (µmol/kgsw)
y = 0.0006x + 2.032
R² = 0.59
B
B/Ca (µmol/mol)
DIC (µmol/kgsw)
y = -0.28x + 1045.9
R² = 0.58
C
B/Ca (µmol/mol)
Net calcification (wt% / 60d)
y = 8.81x + 396
R² = 0.40

838

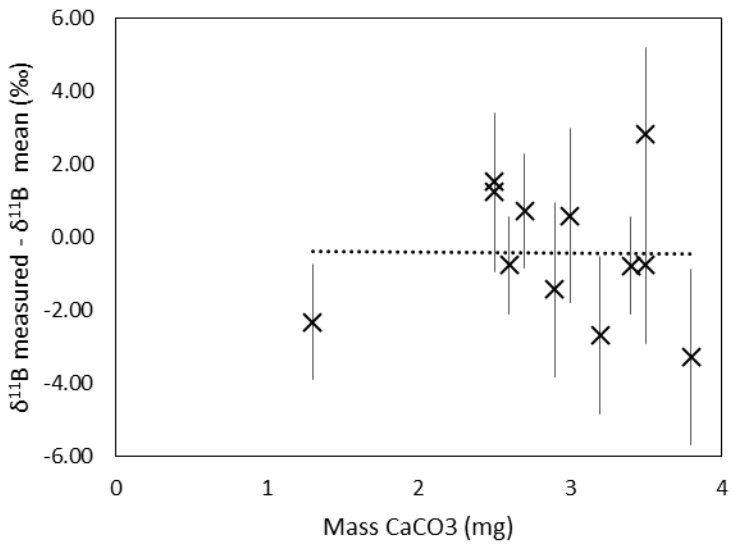
6.00
4.00
2.00
0.00
-2.00
-4.00
-6.00
0
1
2
3
4
δ11B measured - δ11B mean (‰)
Mass CaCO3 (mg)

839

840